Meal detection based on non-individualized moving horizon estimation and classification

Konstanze Kölle[1,2], Anders Lyngvi Fougner[1,2] and Øyvind Stavdahl[1]

***Abstract*— Meals are one of the greatest challenges to glucose regulation in diabetes mellitus type 1. Several times each day, food causes heavily elevated blood glucose concentrations that may result in long-term complications. Meal-time insulin boluses are administered to mitigate these hyperglycemic periods. Sporadic omissions of prandial boluses impair the outcome of the insulin therapy by leading to significant variations in blood glucose levels. As continuous glucose monitoring (CGM) becomes more common, an automated detection based on CGM data could support patients by reminding about missed boluses. In fully automated systems, meal detection could temporarily modify controller parameters until the meal is mitigated. In the present study, moving horizon estimation (MHE) and linear discriminant analysis (LDA), abbreviated "MHE+LDA", are proposed for meal detection. An augmented version of Bergman's minimal model is used for the estimator model. Neither the model parameters nor the MHE tuning are individualized. The method is tested in simulations on the UVa/Padova simulator and its performance is compared to two other methods, namely threshold checking of the current estimated glucose appearance and the GRID algorithm. All meals are detected by MHE+LDA within 35 min while the two comparative methods do not detect the smallest simulated meal. The combination of MHE and LDA outperforms the two other methods also with respect to time of detection. The MHE+LDA method's ability to identify even smaller meals without the need for individual tuning suggests that the method should be further investigated.**

I. INTRODUCTION

THE natural insulin secretion is destroyed in diabetes mellitus type 1 (DM1). Thus, exogenous insulin is usually administered into the subcutaneous (SC) tissue to achieve acceptable blood glucose levels (BGL). The basal insulin needs are covered by either manual injections of long-lasting insulin with insulin pens, or continuous infusion of short-acting insulin from an insulin pump. In both cases, meal time boluses of short-acting insulin are necessary to avoid large BGL excursions. Both size and timing of these boluses influence the effectiveness in normalizing BGL. However, it is rather difficult to estimate the suitable bolus size [1], and patients sometimes even forget administering the bolus. In particular, adolescents tend to omit their diabetes care [2]. Skipped meal-time boluses result in elevated BGL and increase the risk of subsequent over-dosing in an effort to quickly lower the BGL. Formulas relating the amount of carbohydrates and the expected effect of insulin help the patient in estimating the bolus size. Such bolus calculators are also integrated in insulin pumps [3]. A system that automatically detects missed meal boluses and reminds the patient could increase the safety and convenience of DM1 treatment further.

Sensors placed in the SC tissue provide continuous glucose monitoring (CGM) with typical sampling intervals of 1 to 5 min. A meal can be detected if the measured glucose concentration rises above a certain threshold. Measurement noise can be handled by using a Kalman filter (KF) estimate of the glucose concentration rather than the raw CGM signal, see e.g. [4]. Combinations of subsequent threshold violations of the estimated glucose concentration and its rate of change have been proposed to increase the specificity [4], [5], [6]. The KF requires linear models whereas extended (EKF) and unscented Kalman filters (UKF) are designed for the use of non-linear models which may even describe the glucose dynamics in the human body. The UKF using an extended version of Bergman's minimal model [7] has been proposed for meal detection where not the estimated glucose concentration but rather the estimated glucose rate of appearance in plasma is checked against a threshold [8]. Defining the thresholds is in any case a trade-off between sensitivity and specificity. This issue is complicated by the fact that not only short-term perturbations like meals may occur but that the glucose-insulin dynamics, the insulin sensitivity, may vary between and within days.

This paper investigates moving horizon estimation (MHE) with subsequent linear discriminant analysis (LDA), abbreviated "MHE+LDA", for meal detection in DM1. Both MHE and LDA are briefly outlined and motivated in section II. A simulation study that applies the proposed methods is presented in section III and discussed in section IV. The conclusion and future work follow in section V.

II. METHODS

A. Moving Horizon Estimation

A set of ordinary differential equations (ODEs) describes the glucose-insulin dynamics:

$$\dot{\boldsymbol{x}}(t) = \tilde{\boldsymbol{f}}(\boldsymbol{x}(t), \boldsymbol{u}(t)) \tag{1a}$$

$$\boldsymbol{y}(t) = \boldsymbol{h}(\boldsymbol{x}(t)) \tag{1b}$$

with the vectors of differential states $\boldsymbol{x} \in \mathbb{R}^{n_x}$, inputs $\boldsymbol{u} \in \mathbb{R}^{n_u}$, and outputs $\boldsymbol{y} \in \mathbb{R}^{n_y}$.

Moving horizon estimation is a model-based technique similar to model predictive control (MPC) [9], [10]. The current states $\boldsymbol{x}_k$ are estimated based on N past measurements $\{\boldsymbol{y}_{k-N+1}, ..., \boldsymbol{y}_k\}$, instead of predicting the future states $\boldsymbol{x}_{k+1}$ based on the current measurement as in MPC.

[1] Department of Engineering Cybernetics, Norwegian University of Science and Technology - NTNU, Trondheim, Norway {konstanze.koelle, anders.fougner, oyvind.stavdahl}@ntnu.no

[2]Central Norway Regional Health Authority, Trondheim, Norway

The degrees of freedom in MHE are thus the state estimates $\{\boldsymbol{x}_{k-N+1}, ..., \boldsymbol{x}_k\}$ while the historical control variables $\{\boldsymbol{u}_{k-N}, ..., \boldsymbol{u}_{k-1}\}$ are known at time k.

The ODE in eq. (1) was discretized by direct collocation. The discretization allows us to optimize the originally infinite problem as a finite dimensional problem:

$$\underset{\boldsymbol{x}_j, \boldsymbol{w}_j, \boldsymbol{v}_j}{\text{minimize}} \quad J \tag{2a}$$

$$\text{s. t.} \quad \boldsymbol{x}_{j+1} = \boldsymbol{f}(\boldsymbol{x}_j, \boldsymbol{u}_j) + \boldsymbol{w}_j \tag{2b}$$
$$j = k - N + 1, ..., k - 1$$
$$\boldsymbol{y}_j = \boldsymbol{h}(\boldsymbol{x}_j) + \boldsymbol{v}_j \tag{2c}$$
$$j = k - N + 1, ..., k$$
$$\boldsymbol{x}_{j,\min} \leq \boldsymbol{x}_j \leq \boldsymbol{x}_{j,\max} \tag{2d}$$
$$j = k - N + 1, ..., k\,.$$

Unknown disturbances are accommodated by the additive process noise $\boldsymbol{w}_j \in \mathbb{R}^{n_x}$ and the measurement noise $\boldsymbol{v}_j \in \mathbb{R}^{n_y}$.

While minimizing the cost function J, the optimized state values $\boldsymbol{x}_j$ must fulfill the process and measurement equations in (2b) and (2c), respectively. The lower and upper bounds in (2d) constrain the state estimates additionally.

The chosen objective function explicitly considers both process and measurement noise vectors, $\boldsymbol{w}_j$ and $\boldsymbol{v}_j$:

$$J = \|\boldsymbol{x}_{k-N+1} - \bar{\boldsymbol{x}}_{k-N+1}\|^2_{P^{-1}_{k-N+1}} \tag{3a}$$
$$+ \sum_{j=k-N+1}^{k-1} \|\boldsymbol{w}_j\|^2_{R^{-1}} \tag{3b}$$
$$+ \sum_{j=k-N+1}^{k} \|\boldsymbol{v}_j\|^2_{Q^{-1}}\,. \tag{3c}$$

Its first term (eq. (3a)) represents the arrival cost which considers the confidence in the initial estimate $\bar{\boldsymbol{x}}_{k-N+1}$ (first state within the estimation horizon) by means of the estimated error covariance matrix $P_{k-N+1} \in \mathbb{R}^{n_x \times n_x}$. The second and third terms penalize deviations from the process $\boldsymbol{f}(\boldsymbol{x}_j, \boldsymbol{u}_j)$ (eq. (3b)) and the measurement equations $\boldsymbol{h}(\boldsymbol{x}_k)$ (eq. (3c)), respectively.

As time passes, the confidence in the initial state may change as well and the arrival cost needs to be updated. Here, a smoothing update of the initial state $\bar{\boldsymbol{x}}_{k-N+1}$ and its covariance P_{k-N+1} was chosen [11]. By tuning the matrices $R \in \mathbb{R}^{n_x \times n_x}$ and $Q \in \mathbb{R}^{n_y \times n_y}$, the magnitudes of process and measurement noise are weighted.

The non-linear problem was implemented with CASADi [12] in Matlab and solved using IPOPT [13].

B. Classification using linear discriminant analysis

The goal of pattern recognition is to discriminate between different classes within a data set (in this work: "meal onset" and "no meal onset"). First, features need to be selected that are characteristic for the given data set. Features can be any measures or properties of the data. Based on the features, classification algorithms are trained to separate the data into the classes.

Linear discriminant analysis (LDA) is one of the standard classification methods in pattern recognition. In LDA, linear functions are built based on linear combinations of the extracted features and optimized for maximum separation between the classes. A data set with known classification is used to gain the separating functions which then can be applied to classify unknown data sets. The method is described in more detail by e.g. Dougherty [14].

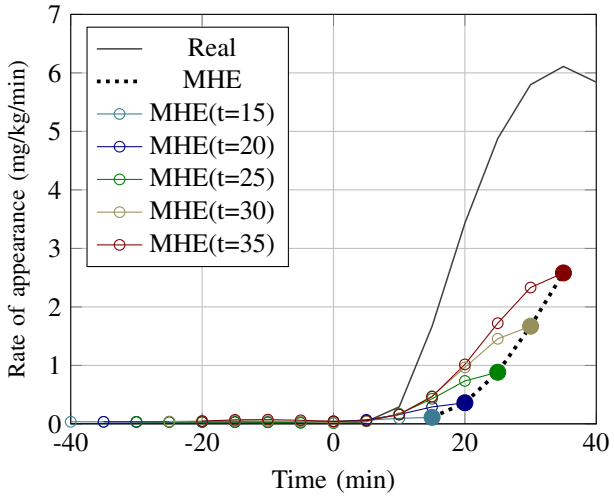

Fig. 1. Glucose rate of appearance estimated by the MHE following a meal at 0 min. Filled circles mark the current estimate at each time step. The dotted line illustrates the estimation using only "current" estimates. Open circles, connected by thin lines, show the horizon estimated in retrospect.

C. Motivation for using moving horizon estimation and linear discriminant analysis for meal detection

Moving horizon estimation has the advantage that constraints on states and parameters are explicitly handled. Both glucose rate of appearance and insulin sensitivity are estimated simultaneously. It is assumed that the insulin sensitivity does not change abruptly but rather drifts over a longer period. Constraints on the respective process noise ensure that the insulin sensitivity changes only gradually. An abrupt change of the glucose concentration as caused by a meal can therefore not be explained by a varying insulin sensitivity. The non-linearity of models is kept in MHE and all measurements within the chosen horizon are considered without linearizing the model at each estimation step or summarizing all measurement information in one state estimate and its covariance, as it is done in KF-type estimators. The result is a whole horizon of estimated past states rather than a single value. Figure 1 illustrates how the estimation becomes more accurate with time if the whole horizon is considered compared to looking at only the current estimate.

The horizon offers additional information that is lost when the detection algorithm checks only the current estimate (filled circles in fig. 1) against some threshold. Linear discriminant analysis considers the characteristic shape of the increasing glucose concentration following a meal.

III. SIMULATION STUDY

A. Estimator model and parameters

The estimator model used in this study is an augmented version of the non-linear model from Bergman et al. [7]. The model has originally been developed to describe the glucose-insulin dynamics during an intravenous glucose tolerance test and has later been used to determine insulin sensitivities during oral glucose loads [15], [16], [17].

The original model has two states: the glucose concentration in plasma G (mg/dL) and the action of insulin X (1/min). We are interested in the rate of appearance of glucose in plasma R_a (mg/kg/min) and thus append R_a to the states as a first order Markov process. The insulin sensitivity S_I (ml/U/min) varies within subjects over time and is therefore estimated simultaneously. However, S_I is assumed constant but subject to noise. The augmented state vector is: $\boldsymbol{x} = [G, X, R_a, S_I]^T$. The following dynamics describe the system:

$$\dot{\boldsymbol{x}}(t) = \begin{bmatrix} -S_G G(t) - X(t)G(t) + S_G G_b + R_a(t)/V_g \\ -p_2 X(t) + p_2 S_I(t)\left(I(t) - I_b\right) \\ -R_a/\tau \\ 0 \end{bmatrix} \tag{4}$$

$$y(t) = G(t)\,. \tag{5}$$

The only measurement y is the glucose concentration in plasma G. Diffusion dynamics of glucose from plasma to the SC tissue is not described in order to restrict the dimensionality of the model. The SC measurements are instead substituted for the plasma concentration in the measurement equation 5. Along the same lines, the absorption of insulin from the SC tissue into the plasma is not modeled but the insulin concentration in plasma I (pmol/L) remains as input. With the motivation of detecting meals, it is assumed that the insulin infusion is close to the basal rate that keeps the glucose concentration stable. On that assumption, the actual value of I has minor impact on the estimation. The basal glucose concentration G_b and the basal insulin concentration I_b in plasma are specific for each subject and given in the simulator. The remaining parameters are not individualized. Descriptions of these generic parameters, the used values and their origin are provided in Table I.

TABLE I

PARAMETER VALUES USED IN THE ESTIMATOR MODEL (EQ. (4)).

Parameter		Description
S_G	$1.4 \cdot 10^{-2}\,\text{min}^{-1}$ [15]	Glucose effectiveness
V_g	1.7 dL/kg [15]	Distribution volume of glucose
p_2	$3.0 \cdot 10^{-2}\,\text{min}^{-1}$ [15]	Rate constant of insulin action
τ	40 min [18]	Meal absorption time constant
$S_{I,\text{nom}}$	$8.56 \cdot 10^{-4}$ ml/U/min [16]	Nominal insulin sensitivity

B. Estimation set-up

A sampling time of 5 min is chosen as it is the most common sampling rate of CGM devices. The optimization problem is constructed at time samples 5 min apart from each other over the whole horizon. These samples are called nodes. The number of nodes in a horizon of e.g. 300 min is thus $N = 300\,\text{min}/5\,\text{min} = 60$.

The initial state (i.e. $\bar{\boldsymbol{x}}_{k-N+1}$ and P^{-1}_{k-N+1} in (3) at $k = 1$) was defined as $\bar{\boldsymbol{x}}_0 = \left[y_0, 10^{-4}, 0, S_{I,\text{nom}}\right]^T$ with an initial covariance $P_0 = I$. The covariance P of the initial state is part of the arrival cost calculation; a smoothing update based on an EKF was chosen [11]. The process and measurement covariances used in this EKF scheme were $\tilde{Q} = \text{diag}\,(10, 10, 1, 1)$ and $\tilde{R} = 100$, respectively. The weighting matrices in the MHE cost function (3) were $Q = \text{diag}\,(50, 10, 10, 1)^2$ for the process noise and $R = 10^2$ for the measurement noise. States and noise vectors were bounded as

$$\begin{bmatrix} \boldsymbol{x}_{\min} \\ \boldsymbol{w}_{\min} \\ \boldsymbol{v}_{\min} \end{bmatrix} \leq \begin{bmatrix} \boldsymbol{x} \\ \boldsymbol{w} \\ \boldsymbol{v} \end{bmatrix} \leq \begin{bmatrix} \boldsymbol{x}_{\max} \\ \boldsymbol{w}_{\max} \\ \boldsymbol{v}_{\max} \end{bmatrix}\,, \tag{6}$$

in which the inequalities should be interpreted elementwise, with

$$\boldsymbol{x}_{\min} = \left[36, -10^{-2}, 0, 0.5 \cdot S_{I,\text{nom}}\right]^T\,, \tag{7a}$$
$$\boldsymbol{x}_{\max} = \left[300, 10^{-2}, 10, 2 \cdot S_{I,\text{nom}}\right]^T\,, \tag{7b}$$
$$\boldsymbol{w}_{\min} = \left[-10^{-4}, -10^{-8}, 0, -10^{-8}\right]^T\,, \tag{7c}$$
$$\boldsymbol{w}_{\max} = \left[10^{-4}, 10^{-8}, \text{inf}, 10^{-8}\right]^T\,, \tag{7d}$$
$$\boldsymbol{v}_{\min} = -10^{8} \quad \text{and} \tag{7e}$$
$$\boldsymbol{v}_{\max} = 10^{8}\,. \tag{7f}$$

C. Methods for meal detection

A meal detection is defined as a true positive (TP) when the meal is detected within 60 min after the onset. All instances of detection out of this period are consequently regarded as false positives (FP). Series of consecutive TPs are counted as a single TP instance. Likewise, any number of consecutive FPs are counted as one single FP detection. A false negative (FN) detection occurs if the meal is not detected within a period of 60 min after the meal onset. All other instances without detection are true negative (TN) but not explicitly counted here.

Three methods for meal detection are compared.

1) Threshold on R_a-estimate: The first method checks the current R_a estimate from the MHE against a threshold. The current estimate at each time step corresponds to the last value in the horizon. In a study using UKF, meals of various glucose content are detected if the estimated glucose rate of appearance exceeded 2 mg/dL/min [8]. This threshold is used after adjusting the units to $2\,\text{mg/dL/min} \cdot V_g = 3.4\,\text{mg/kg/min}$.

2) GRID algorithm: Secondly, we apply the Glucose Rate Increase Detector (GRID) by Harvey et al. [6] to the glucose measurements. The GRID algorithm is used with the tuning reported in [6].

3) MHE+LDA: The two previously listed methods serve as comparison for our meal detection using MHE+LDA.

Linear discriminant analysis (section II-B) is applied to the estimated R_a-horizons from MHE. The classifier is trained on simulated data from 3 distinct meals applied to each of the 10 adult subjects, yielding a total of 30 simulated single meals. The three meals have a carbohydrate content of 25, 50 and 75 g, respectively, and last for 15 min. The last 20 nodes of the R_a-horizons, i.e. a period of the most current 100 min, are used for detection. A horizon with a meal onset falling within the horizon's most current 60 min, i.e. the horizon ends no later than 60 min after meal onset, is designated to the class "meal onset", all others are assigned to the class "no meal onset". That ensures that the classification is trained to detect the onset of meals. The LDA based on MHE estimations is tested in a leave-one-out cross-validation for those 30 meals. The detection algorithm is started as soon as the full horizon length is reached.

D. Estimation on data simulated with estimator model

In a first scenario, a meal is simulated by feeding a trajectory of glucose rate of appearance as input into the estimator model, thereby generating a glucose concentration. The resulting glucose concentration is used as measurement in the MHE that estimates R_a again. The initial R_a-trajectory was generated with the UVa/Padova simulator simulating a meal with carbohydrate content of 50 g in adult subject 1.

An oscillating insulin sensitivity with a period of 1440 min was simulated as follows:

$$S_I(t) = S_{I,\text{nom}} + 0.5 \cdot S_{I,\text{nom}} \cdot \sin(2\pi t/1440\,\text{min})\,. \quad (8)$$

This corresponds to an insulin sensitivity that is changing from its nominal value by ±50% within 6 hours, which appears realistic [19].

In addition, an oscillating insulin concentration in plasma was simulated with a period of 360 min:

$$I(t) = I_b + 20 \cdot \sin(2\pi t/360\,\text{min})\,. \quad (9)$$

Figure 2 illustrates the current estimate of the MHE for different horizons for a simulation where Gaussian white noise with a variance of $\sigma^2 = 2\,(\text{mg/dL})^2$ was superimposed to the simulated glucose measurements. The estimates for the shortest horizon of 60 min are more noisy than the estimates for the longer horizons which do not differ significantly.

Figures 3 and 4 show the estimations of insulin action and insulin sensitivity for simulations without additional measurement noise. The estimated insulin action in fig. 3 follows the simulated oscillations well. Longer horizons are again beneficial for the accuracy. There is a larger deviation between the estimates of the insulin sensitivity and the simulated data in fig. 4. Opposite to R_a and X, a shorter horizon leads to more accurate estimations of the insulin sensitivity. The reason is that S_I is constant within one estimated horizon due to the modeling in (4) (not shown). Any changes can only origin from the added process noise in the MHE formulation (2b). For the purpose of meal detection, an accurate R_a-estimate is more important than

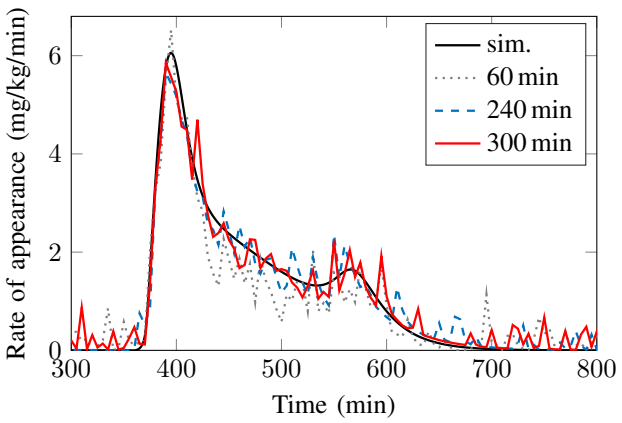

Fig. 2. Comparison of estimated glucose rate of appearance R_a for different MHE horizons in a scenario where R_a mimics a meal starting at 360 min. (R_a-trajectory generated with UVa/Padova simulator, simulated as input into estimator model, random measurement noise added).

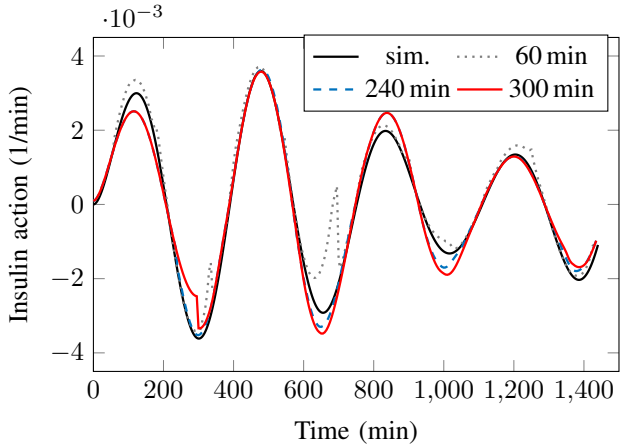

Fig. 3. Comparison of estimated insulin action (X) for different MHE horizons in a scenario where insulin concentration in plasma (I) was set as a sinusoid signal. Insulin actions below zero appear due to the simplified model. Negative insulin action can be interpreted as the glucose-increasing effect of the hormone glucagon that releases glucose from the liver.

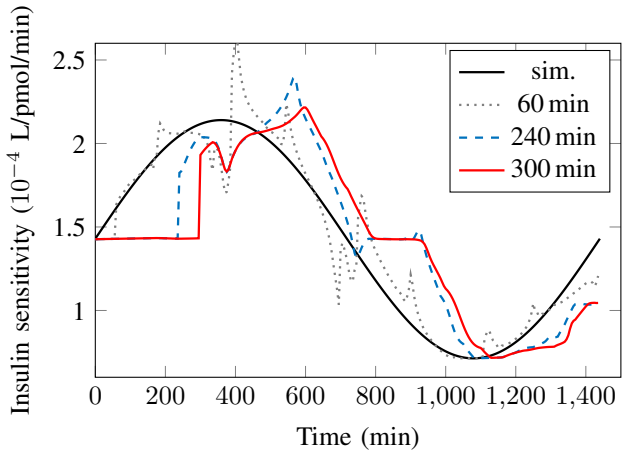

Fig. 4. Comparison of estimated insulin sensitivity (S_I) for different MHE horizons in a scenario where insulin sensitivity was set as a sinusoid signal. Insulin sensitivity stays at its nominal value until the horizon has reached full length and both the initial value and covariance change.

a good approximation of insulin sensitivity, and therefore, a horizon of 300 min is chosen in this work.

E. Estimation on data simulated with UVa/Padova simulator

The proposed MHE+LDA method for meal detection is tested on simulated measurement data generated with the academic version of the UVa/Padova T1DM simulator from 2013. The simulator model describes the glucose-insulin metabolism in man with DM1 [20] with higher complexity than the estimator model. This mimics the differences between an estimator model and the real metabolism. Open loop scenarios of single meals are simulated in 10 adult subjects. The subjects are controlled at their basal glucose concentration before the meals start. This is achieved by administering insulin continuously at the subject-specific basal rate defined in the simulator. The basal rate is injected during the whole experiment without superimposed insulin boluses.

Single-meal scenarios with a carbohydrate content of 25, 50 and 75 g are simulated for the ten adult subjects. All meals last for 15 min regardless of their carbohydrate content. An error-free pump and the sensor Freestyle Navigator (Abbott Diabetes Care, Alameda, CA) with a partial auto-correlation coefficient (PACF) of 0.25 is used in all simulations. An example of all three meal sizes for one subject their detection by MHE+LDA is shown in fig. 5.

Table II summarizes the detection with MHE+LDA and with the two comparative methods (described in section III-C) for each meal size. The results for the meal with a carbohydrate content of 50 g are separately listed for each subject in table III. The sensed glucose concentration and the times of detection for subject 7 are shown additionally in fig. 6. The MHE+LDA detects all 30 meals within a maximum of 35 min after their onset. Two false positive detections occur with MHE+LDA 90 min after the meal, one for subject 7 after a meal with 50 g and one for subject 5 following a meal with 75 g.

IV. DISCUSSION

In both cases of false positive detections with MHE+LDA, the glucose concentration is still rising when the "false" detection occurs. Figure 6 illustrates this for the 50 g-meal in subject 7. If the period, in which a detection is accepted as true positive, was extended to e.g. 90 min, neither of the FP would appear in the statistics. In practice, the detection of a new meal could be suspended until the effect of injected insulin has settled to avoid detecting the same meal several times and possibly triggering the infusion of too much insulin. Another possibility to avoid the two reported FP in table II is to extend the postprandial period that is defined as "meal onset" in the training set. No FP would occur, for example, if data from horizons estimated up to 90 min after the meal onset were included. The smallest meals would then be detected on average 6.5 min later, so it is a trade-off between detection times and rates of false positives. The best option is possibly to define the training data depending on the meal size.

While MHE+LDA can detect meals of all sizes used in this study, neither the GRID algorithm nor the threshold check is able to detect the smallest meal of 25 g carbohydrates. This result is not surprising as the GRID algorithm was tuned for meals from 50 g upwards [6]. On the other hand, the GRID algorithm shows no FP detection. A different tuning of the GRID algorithm has not been tested here.

A lower threshold on the current estimate increases the sensitivity of the threshold check to smaller meals. All 25 g-meals are detected with a halved threshold of $R_{a,\text{th}} = 1.7\,\text{mg/kg/min}$, for example. The detection with MHE+LDA still outperforms the threshold check in this scenario with respect to early detection as the meals are on average detected 5 min earlier. Moreover, eight FP occur with the halved threshold only for the smallest meals (compared to zero with full threshold), illustrating the obvious fact that the risk of false positives increases with lower thresholds.

All FP with the threshold check occur after the meal. Most of them (9 of 14) appear while the glucose concentration is still increasing after a meal as discussed above. The remaining five FP occur in the period with decreasing glucose concentrations after a 75 g-meal due to poor R_a-estimations. The reason could be that the MHE has been tuned for a meal of 50 g in subject 1 and performs less well for the other subjects. The related R_a-horizons could also be less accurate because of an inappropriate meal model in the third subequation of eq. (4). However, the LDA in MHE+LDA overcomes this issue by focusing on the meal onset.

The tuning of the optimization problem in the MHE is complex and was partly found by trial and error for one meal size in one subject. A slightly different tuning may lead to different results. Future work should thus explore the possibilities for robust, automatic tuning. The sampling rate of 5 min restricts the detection opportunities to every 5 min. A more frequent detection might be achievable with higher sampling frequency.

Glucose measurements were generated with a simulation model that is more complex than the one used in the estimator. The parameters in the estimator model were not adjusted to individual subjects. Thus, the results are promising as the MHE with subsequent LDA detects all meals and at an earlier time than the compared methods. Individualization of model parameters could be investigated as it may improve the performance further, though the fact that the method might not require individualization is definitely a strength with respect to the applicability in clinical practice.

The estimator model in eq. (4) describes the glucose-insulin dynamics in blood plasma, although the CGM device and the insulin injection are usually located in the SC tissue. Equations for insulin absorption to and glucose diffusion from the plasma are omitted in this study to restrict the number of uncertain parameters. The results indicate that a model of glucose diffusion is not necessary because all meals are successfully detected by just substituting the glucose concentration in plasma by SC CGM data.

No insulin bolus or closed-loop scenario is simulated in this study. In order to do that, MHE would need to

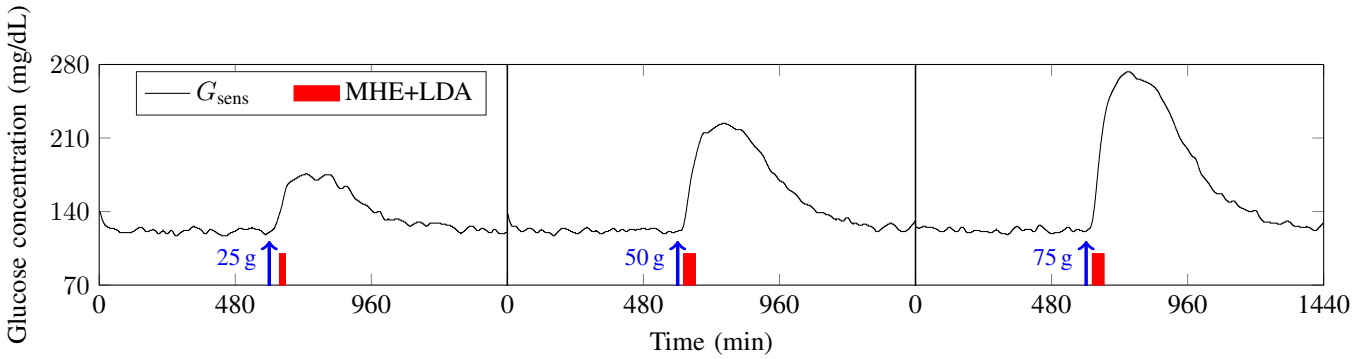

Fig. 5. Sensed glucose concentration for meals with different carbohydrate content for one subject. Red bars indicate detection by MHE+LDA.

TABLE II

RESULTS OF DETECTION OF MEALS WITH DIFFERENT SIZES USING DIFFERENT METHODS: (1) THRESHOLD CHECK ON LAST R_a-ESTIMATE FROM MHE ($R_{a,\text{TH}} = 3.4$ MG/KG/MIN), (2) GRID ALGORITHM [6] AND (3) MHE WITH SUBSEQUENT LDA ON R_a-ESTIMATES. [1]

	Threshold on R_a-estimate				GRID algorithm [6]				MHE+LDA			
Meal size	Δt_{Det} (min)	ΔG_{Det} (mg/dL)	FP	FN	Δt_{Det} (min)	ΔG_{Det} (mg/dL)	FP	FN	Δt_{Det} (min)	ΔG_{Det} (mg/dL)	FP	FN
25 g	-	-	0	10	-	-	0	10	26.0 (4.9)	10.1 (5.1)	0	0
50 g	32.2 (4.8)	30.1 (5.4)	6	1	41.1 (5.2)	48.6 (6.4)	0	1	19.5 (3.5)	6.4 (2.9)	1	0
75 g	26.5 (3.9)	26.6 (6.1)	8	0	35 (3.2)	53.6 (9.1)	0	0	18.5 (2.3)	7.7 (2.4)	1	0

[1] Δt_{Det}: time of detection after meal onset, ΔG_{Det}: glucose deviation from basal at detection, FP: false positives, FN: false negatives. Average (standard deviation) of Δt_{Det} and ΔG_{Det}, total number of FP and FN for all 10 subjects.

TABLE III

RESULTS OF DETECTION OF A 50 G-MEAL USING DIFFERENT METHODS: (1) THRESHOLD CHECK ON LAST R_a-ESTIMATE FROM MHE ($R_{a,\text{TH}} = 3.4$ MG/KG/MIN), (2) GRID ALGORITHM [6] AND (3) MHE WITH SUBSEQUENT LDA ON R_a-ESTIMATES. [1]

	Threshold on R_a-estimate				GRID algorithm [6]				MHE+LDA			
	Δt_{Det} (min)	ΔG_{Det} (mg/dL)	FP	FN	Δt_{Det} (min)	ΔG_{Det} (mg/dL)	FP	FN	Δt_{Det} (min)	ΔG_{Det} (mg/dL)	FP	FN
Subject 1	35	38.1	1	0	45	58.5	0	0	20	7.1	0	0
Subject 2	25	22.7	0	0	35	45.0	0	0	15	3.5	0	0
Subject 3	-	-	0	1	-	-	0	1	25	10.9	0	0
Subject 4	35	27.4	0	0	45	43.2	0	0	20	4.7	0	0
Subject 5	35	35.6	2	0	40	43.2	0	0	20	8.1	0	0
Subject 6	30	25.7	0	0	40	50.9	0	0	20	6.5	0	0
Subject 7*	25	25.7	1	0	35	56.8	0	0	15	3.9	1	0
Subject 8	35	30.4	1	0	45	49.1	0	0	20	5.2	0	0
Subject 9	30	27.2	1	0	35	38.1	0	0	15	2.6	0	0
Subject 10	40	38.0	0	0	50	52.6	0	0	25	11.4	0	0

[1] Δt_{Det}: time of detection after meal onset, ΔG_{Det}: glucose deviation from basal at detection, FP: false positives, FN: false negatives.

* The meal detection for subject 7 is shown in fig. 6.

be informed about insulin doses that are administered in addition to the basal dose, and then the estimator model would need to be extended with the insulin absorption from the SC tissue into blood. This may prove to be beneficial if it increases the accuracy of the MHE estimates.

Meal detection by MHE+LDA may be improved using simulations with extended scenarios including insulin boluses and more severe perturbations. As LDA may prove

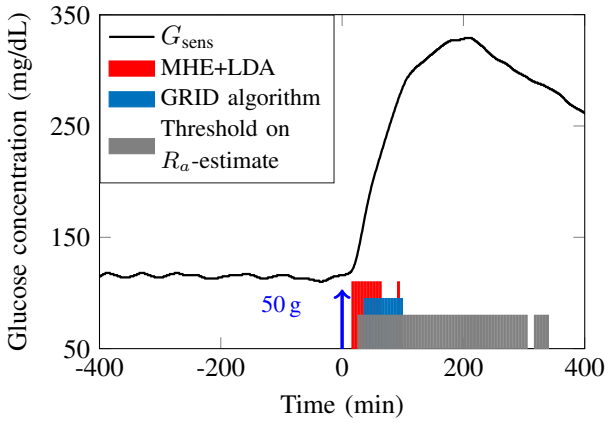

Fig. 6. Sensed glucose concentration for meal with 50 g carbohydrates at 0 min for subject 7 and instances of detection with different methods.

to be less precise, other methods of pattern recognition than LDA can be exploited. Finally, the method should be validated on clinical data.

V. CONCLUSION

All simulated single meals are detected with the LDA based on the estimated horizons of the glucose rate of appearance. Compared to threshold checking on an estimated glucose appearance and the GRID algorithm, meals are detected significantly earlier with only a few false detections. These false detections only occur in non-critical situations that are per se still during the meal and can be avoided easily by slightly redefining the marking of "meal onset" in the training data of the LDA, or be silenced by a logic handling the detections. Neither the minimal estimator model nor the MHE needs individually tuned parameters to achieve this result in the simulated cases. Meal detection using MHE+LDA should therefore be tested on real CGM data in order to further investigate its suitability.

ACKNOWLEDGMENT

The authors thank Professor Morten Hovd and Leif Erik Andersson for valuable discussions about the moving horizon estimation. Leif Erik Andersson also contributed with practical advice on the implementation using CASADi.

REFERENCES

[1] A.S. Brazeau, H. Mircescu, K. Desjardins, *et al.*, "Carbohydrate counting accuracy and blood glucose variability in adults with type 1 diabetes," *Diabetes Res Clin Pract*, vol. 99, no. 1, pp. 19–23, 2013.

[2] A.L. Olinder, K.T. Nyhlin, and B. Smide, "Reasons for missed meal-time insulin boluses from the perspective of adolescents using insulin pumps: 'lost focus'.(report)," *Pediatric Diabetes*, vol. 12, no. 4pt2, p. 402, 2011.

[3] H. Zisser, L. Robinson, W. Bevier, *et al.*, "Bolus calculator: A review of four smart insulin pumps," *Diabetes Technol Ther*, vol. 10, no. 6, pp. 441–444, 2008.

[4] E. Dassau, B.W. Bequette, B.A. Buckingham, *et al.*, "Detection of a meal using continuous glucose monitoring implications for an artificial β-cell," *Diabetes care*, vol. 31, no. 2, pp. 295–300, 2008.

[5] H. Lee and B.W. Bequette, "A closed-loop artificial pancreas based on model predictive control: Human-friendly identification and automatic meal disturbance rejection," *Biomed Signal Process Control*, vol. 4, no. 4, pp. 347–354, 2009.

[6] R.A. Harvey, E. Dassau, H. Zisser, *et al.*, "Design of the glucose rate increase detector a meal detection module for the health monitoring system," *J Diabetes Sci Technol*, p. 1932296814523881, 2014.

[7] R.N. Bergman, L.S. Phillips, and C. Cobelli, "Physiologic evaluation of factors controlling glucose tolerance in man: measurement of insulin sensitivity and beta-cell glucose sensitivity from the response to intravenous glucose," *The Journal of clinical investigation*, vol. 68, no. 6, p. 1456, 1981.

[8] K. Turksoy, S. Samadi, J. Feng, *et al.*, "Meal detection in patients with type 1 diabetes: A new module for the multivariable adaptive artificial pancreas control system," *IEEE Trans. Biomed. Eng.*, vol. 20, no. 1, pp. 47–54, 2016.

[9] M. Diehl, H.J. Ferreau, and N. Haverbeke, "Efficient numerical methods for nonlinear MPC and moving horizon estimation," in *Nonlinear model predictive control*. Springer, 2009, pp. 391–417.

[10] P. Kühl, M. Diehl, T. Kraus, *et al.*, "A real-time algorithm for moving horizon state and parameter estimation," *Computers & Chemical Engineering*, vol. 35, no. 1, pp. 71–83, 2011.

[11] M.J. Tenny and J.B. Rawlings, "Efficient moving horizon estimation and nonlinear model predictive control," in *Proceedings of the 2002 American Control Conference*, vol. 6, 2002, pp. 4475–4480.

[12] J. Andersson, "A general-purpose software framework for dynamic optimization," PhD Thesis, Arenberg Doctoral School, KU Leuven, 2013.

[13] A. Wächter and L.T. Biegler, "On the implementation of an interior-point filter line-search algorithm for large-scale nonlinear programming," *Mathematical Programming*, vol. 106, no. 1, pp. 25–57, 2006.

[14] G. Dougherty, *Pattern Recognition and Classification : An Introduction*. Springer New York, 2013.

[15] C. Dalla Man, A. Caumo, and C. Cobelli, "The oral glucose minimal model: estimation of insulin sensitivity from a meal test," *IEEE Trans. Biomed. Eng.*, vol. 49, no. 5, pp. 419–429, 2002.

[16] C. Dalla Man, A. Caumo, R. Basu, *et al.*, "Minimal model estimation of glucose absorption and insulin sensitivity from oral test: validation with a tracer method," *American journal of physiology. Endocrinology and metabolism*, vol. 287, no. 4, p. E637, 2004.

[17] L. Hinshaw, C. Dalla Man, D.K. Nandy, *et al.*, "Diurnal pattern of insulin action in type 1 diabetes: implications for a closed-loop system," *Diabetes*, vol. 62, no. 7, p. 2223, 2013.

[18] R. Hovorka, V. Canonico, L.J. Chassin, *et al.*, "Nonlinear model predictive control of glucose concentration in subjects with type 1 diabetes," *Physiological measurement*, vol. 25, no. 4, p. 905, 2004.

[19] R. Visentin, C. Dalla Man, Y.C. Kudva, *et al.*, "Circadian variability of insulin sensitivity: Physiological input for in silico artificial pancreas," *Diabetes Technology and Therapeutics*, vol. 17, no. 1, pp. 1–7, 2015.

[20] C. Dalla Man, F. Micheletto, D. Lv, *et al.*, "The UVA/Padova type 1 diabetes simulator: New features," *J Diabetes Sci Technol*, vol. 8, no. 1, pp. 26–34, 2014.